Pseudopotential and all-electron atomic core size scales

Alex Zunger

Citation: The Journal of Chemical Physics **74**, 4209 (1981); doi: 10.1063/1.441556
View online: http://dx.doi.org/10.1063/1.441556
View Table of Contents: http://scitation.aip.org/content/aip/journal/jcp/74/7?ver=pdfcov
Published by the AIP Publishing

Pseudopotential and all-electron atomic core size scales

Alex Zunger

Solar energy Research Institute, Golden, Colorado 80401
(Received 28 October 1980; accepted 20 November 1980)

It has recently been shown by Politzer and Parr,[1] Boyd,[2] and Politzer[3] (denoted here PPB), following the work of Weinstein *et al.*[4] that whereas for any ground state atom with $Z>2$, the spherically symmetric all-electron Hartree–Fock (HF) charge density $\rho(r)=\sum_{nl} N_{nl}|\psi_{nl}(r)|^2$ is a monotonically decreasing function of r, the *radical* charge density $R(r)=4\pi r^2\rho(r)$ has at least one minimum. The position r_m of the outermost minimum of $R(r)$ was shown to vary systematically and monotonically along rows (but not columns) of the Periodic Table and to constitute a chemically meaningful atomic index delineating the core ($r<r_m$) region from the valence ($r>r_m$) region of the atom. The uniqueness and significance of the new core size coordinates (r_m) is highlighted by the fact that a Thomas–Fermi calculation of the total valence energy of atoms $E_v(r_m)$ correctly predicts the trends and often the magnitude of the spectroscopically observed E_v values only if r_m is used as an inner cutoff for the potential integration, whereas other choices produce large deviations.[1]

The physicist's view of the partitioning of coordinate or momentum space into nonpenetrating core and valence regions is more often based on the notion of the pseudopotential[5] $V_{ps}^{(l)}(\mathbf{r})$: This is the external potential which, when added to the potential produced by the valence electrons {i.e., the screening potential $W_{scr}[n(r)]$} in atoms, molecules, or solids, correctly replaces the dynamic effects of the core wavefunctions. As pseudo wave functions are nodeless for each of the lowest angular momentum (l) states, the information contained in the PPB type core radii (r_m) is no longer encoded in the radial *pseudo* charge density $R_{ps}(r)=4\pi r^2 n(r)$. In turn, the information is transferred to $V_{ps}^{(l)}(\mathbf{r})$ through the pseudopotential transformation mapping the all-electron density $\rho(r)$ onto the pseudo charge density $n(r)$.[5]

The angular-momentum-dependent delineation between the core and valence regions would be faithfully encoded in $V_{ps}^{(l)}(\mathbf{r})$ if it were calculated from the all-electron orbitals $[\psi_{nl}(r)]$ and potential $V(r)$ in a systematic and *a priori* manner. However, pseudopotentials used in solid-state applications are usually generated by empirically fitting a selected subset of orbital energies (of ions[6] or interband transitions in semiconductors[7] or Fermi surfaces of metals[8]), without constraining the pseudo wave functions to reproduce the tails of the true orbitals, whereas pseudopotentials used in quantum chemical calculations (e.g., Ref. 9) are often constructed merely to achieve computational simplification of the otherwise time consuming all-electron calculations. Indeed, the inherent nonuniqueness of the pseudo-wave functions[5] allows a certain arbitrariness in constructing pseudopotentials, a freedom which has been often utilized to achieve analytic simplicity or computational ease, sacrificing the details of $V_{ps}^{(l)}(\mathbf{r})$ in the small-r core regions as well as the systematic regularities of $V_{ps}^{(l)}(\mathbf{r})$ as a function of atomic number.

Recently,[10] *a priori* atomic pseudopotentials have been developed for all atoms of the first five rows of the Periodic Table by using an extension of the density-functional Kohn and Sham formalism.[11] The shape of the pseudopotential is not arbitrarily fixed from the outset, nor is it determined by a fitting procedure. Instead, its form over all space is dictated by representing the atomic pseudo orbitals as a rotation in the subspace of the occupied all-electron orbitals $[\psi_{nl}(r)]$. A specific method of constructing the rotation matrix eliminates the underlying wave function nonuniqueness by imposing a set of arbitrary but physically significant constraints. These pseudopotentials have been used successfully in self-consistent electronic structure calculations[10,12,13] for atoms, simple molecules, bulk semiconductors, transition metals, and semiconductor surfaces and interfaces, as well as for calculation of cohesive properties of solids.

The significance of these pseudopotentials to the present discussion is that the screened pseudopotentials (i.e., the total effective potential sampled by an electron in a pseudoatom) $V_{eff}^{(l)}(r)=V_{ps}^{(l)}(r)+W_{scr}[n(r)]+l(l+1)/2r^2$ are characterized by the crossing points r_l at which $V_{eff}^{(l)}(r)$ has its only node, and that the set $\{r_l\}$ forms an internal, *orbitally dependent* distance scale delineating the repulsive $[V_{eff}^{(l)}(r)>0]$ core region ($r<r_l$) from the attractive $[V_{eff}^{(l)}(r)<0]$ valence region ($r>r_l$). (Here $W_{scr}[n]$ denotes the Coulomb exchange and correlation screening due to the valence electrons, and $l/(l+1)/2r^2$ is the centrifugal potential.) The pseudopotential orbital radii $\{r_l\}$ can be viewed as a quantum mechanical realization of the isotropic semiclassical atomic radii used extensively in structural chemistry and crystallography[14]: r_s scales linearly with Pauling's tetrahedral radii; r_p scales with Ashcroft's[8] empty-core radii; (r_s+r_p) is linear with respect to Pauling's univalent radii; and r_l^{-1} scales linearly with the multiplet-averaged experimental ionization energy E_l of the lth orbital.[14] However, even more spectacular is the way in which the indices r_s and r_p can be used to predict the stable crystal structure of all binary AB-type (stoichiometric and ordered) compounds (a total of 565 crystals whose atoms belong to the first five rows of the periodic table for which $\{r_l\}$ values have been calculated[14,15]). Following St. John and Bloch,[16] Machlin, Chow, and Phillips,[17] and Chelikowsky and Phillips,[18] we define for each AB crystal the dual structural coordinates $R_\sigma^{AB}=|(r_p^A+r_s^A)-(r_p^B+r_s^B)|$ and $R_\pi^{AB}=|r_p^A-r_s^A|+|r_p^B-r_s^B|$. The striking observation is that in the R_σ^{AB} vs R_π^{AB} plane there exists a set of simple straight lines that delineate with

 0021-9606/81/074209-03$01.00

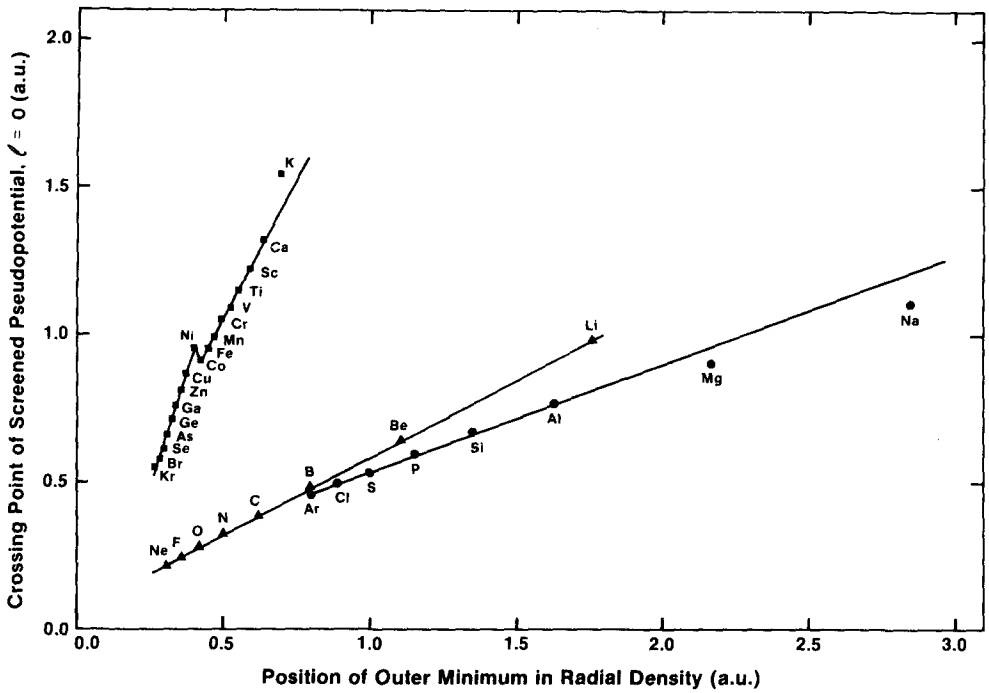

FIG. 1. Linear correlation between the $l=0$ component of the pseudopotential radii[14] and the PPB core radii.[3]

remarkable accuracy regions belonging to experimentally distinct crystallographic structural domains.[15]

In this Note, I point to the existence of a remarkably accurate phenomenological linear dependence between the PPB core radii $\{r_m\}$ and the $l=0$ component of the pseudopotential orbital radii $\{r_s\}$. This relation is shown in Fig. 1 for all atoms for which r_m values have been published.[1-3] (Values of $[r_l;\ l=0,1,2]$ for 70 atoms are given in Table I of Ref. 14.) In addition, I show that the PPB core radii scale linearly with the radius $\{r^s_{nd}\}$ at which the s-like HF valence orbital has its outer node (Fig. 2). (Values for r^s_{nd} are taken from Ref. 19.) These remarkable scaling relationships suggest the universality of these quantum mechanical scales for atomic core radii. The significance of this finding is emphasized by the fact that the radii $\{r_m, r^s_{nd}\}$ are obtained through physical models (all-electron HF orbitals and radial densities) that are vastly different from the models used for constructing the $\{r_l\}$ radii (pseudopotentials in a density-functional formalism, including homogeneous electron gas correlation corrections). Furthermore, the scaling of $\{r^s_{nd}\}$ with the bond length of simple metals and transition metals and with the average interelectronic spacing in solids[20] establishes $\{r^s_{nd}\}$ as a transferable atomic size scale, underlying solid state interactions.

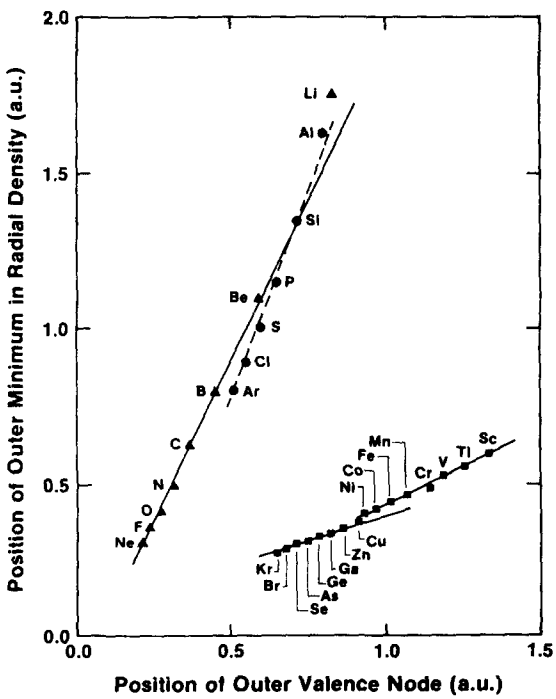

FIG. 2. Linear correlation between the outer node position in the s-like HF valence orbitals (Ref. 19) and the PPB radii (Ref. 3). The first two atoms in rows 2 and 3 of the Periodic Table (Na, Mg, K, Ca) deviate from this correlation.

The significant difference between these two sets of scales remains that at present the PPB radii (constructed from total densities rather than from individual wave functions) do not resolve the core coordinates into angular momentum components and therefore cannot be used to assess structural regularities in the manner described above for $\{r_l\}$.[14-18] Furthermore, unlike the $l=0$ and $l=2$ coordinates, the outer node radii r^l_{nd} (or the average node positions) for $l=1$ do not scale regularly with the pseudopotential radii r_p.[14] Consequently, the *structural* information encoded in $\{r_l\}$ is not contained in either $\{r_m\}$ or $\{r^s_{nd}\}$.

[1] P. Politzer and R. G. Parr, J. Chem. Phys. **64**, 4634 (1976).
[2] R. J. Boyd, J. Chem. Phys. **66**, 356 (1977).
[3] P. Politzer, J. Chem. Phys. **72**, 3027 (1980).

[4]H. Weinstein, P. Politzer, and S. Serbernik, Theor. Chem. Acta **38**, 159 (1975).
[5]J. C. Phillips and L. Kleinman, Phys. Rev. **116**, 287 (1959); M. H. Cohen and V. Heine, *ibid.* **122**, 1821 (1961).
[6]I. V. Abarenkov and V. Heine, Phil. Mag. **12**, 529 (1965); L. Szasz and G. McGinn, J. Chem. Phys. **45**, 7898 (1966).
[7]M. L. Cohen and V. Heine, in *Solid State Physics*, edited by H. Ehrenreich, F. Seitz, and D. Turnbull (Academic, New York, 1970), Vol. 24, p. 38.
[8]N. W. Ashcroft, Phys. Lett. **23**, 48 (1966).
[9]V. Bonifacic and S. Huzinaga, J. Chem. Phys. **60**, 2779 (1974); C. S. Ewig and J. R. Van Wazer, *ibid.* **63**, 4035 (1975).
[10]A. Zunger, S. Topiol, and M. Ratner, Chem. Phys. **39**, 75 (1979); A. Zunger and M. L. Cohen, Phys. Rev. B **18**, 5449 (1978); **20**, 4082 (1979); A. Zunger, J. Vac. Sci. Technol. **16**, 1337 (1979).
[11]P. C. Hohenberg and W. Kohn, Phys. Rev. **136**, 864 (1964); W. Kohn and L. J. Sham, *ibid.* **140**, 1133 (1965).
[12]M. Schlüter, A. Zunger, G. P. Kerker, K. M. Ho, and M. L. Cohen, Phys. Rev. Lett. **42**, 540 (1979); G. P. Kerker, A. Zunger, M. L. Cohen, and M. Schlüter, Solid State Commun. **32**, 309 (1979).
[13]A. Zunger and M. L. Cohen, Phys. Rev. B **19**, 568 (1979); A. Zunger, G. P. Kerker, and M. L. Cohen, *ibid.* **20**, 581 (1979); A. Zunger, *ibid.* 21, 4785 (1980); 22, 649, 959 (1980).
[14]A. Zunger, Phys. Rev. B **22**, 5839 (1980).
[15]A. Zunger, Phys. Rev. Lett. **44**, 582 (1980).
[16]J. St. John and A. N. Bloch, Phys. Rev. Lett. **33**, 1095 (1974).
[17]E. S. Machlin, T. P. Chow, and J. C. Phillips, Phys. Rev. Lett. **38**, 1292 (1977).
[18]J. R. Chelikowsky and J. C. Phillips, Phys. Rev. B **17**, 2453 (1978).
[19]J. B. Mann, Los Alamos Scientific Laboratory, Rep. LA-3691 (1968).
[20]M. Natapoff, J. Chem. Solids **37**, 59 (1976); **39**, 1119 (1978).

Electric dipole moment of $KrSO_3$ [a)]

K. R. Leopold, K. H. Bowen,[b)] and W. Klemperer

Department of Chemistry, Harvard University, Cambridge, Massachusetts 02138
(Received 6 October 1980; accepted 9 December 1980)

In a recent study,[1] we determined by molecular beam electric resonance spectroscopy the dipole moments and molecular symmetry of the weakly bound complexes $ArSO_3$ and N_2SO_3. Both of these species were found to have a symmetric top structure in which the Ar atom or N_2 molecule adds along the symmetry axis of the SO_3. Analysis of the radio frequency (Stark) spectra showed the dipole moments to be 0.2676(3)D and 0.46(1)D for $ArSO_3$ and N_2SO_3, respectively.

Here we report the radio frequency spectrum of $^{84}KrSO_3$. A beam of this complex was produced by expanding a mixture of Ar, Kr, and SO_3 at 900 Torr through a 3 m nozzle at 25 °C. The mixture was produced by pulse-injecting[2] pure Kr into a flowing stream of Ar seeded with SO_3. This technique provides a convenient method of controlling the concentration of Kr in the mixture during the experiment. The concentration of Kr was approximately 10%; that of SO_3 is more difficult to estimate.[1] Thirty percent of the straight through beam was focused around a movable beam obstacle by 20 kV on the quadrupolar A field. Spectra were taken monitoring the mass peak of the parent ion $^{84}Kr^{32}S^{16}O_3^+$ ($m/e = 164$) which contains the most abundant Kr, S, and O isotopes, and has zero nuclear spin as well.

The Stark spectrum of $^{84}KrSO_3$ is extremely simple. Due to the absence of off-axis nuclear spin, only the $K = 0, 3, 6\ldots$ levels exist and the transitions $\Delta M_J = \pm 1$ are easily assigned. Table I gives the measured transition frequencies and their assignments. The frequencies fit the normal first-order Stark effect for a symmetric top. The dipole moment obtained from these data is 0.369(2)D. The more complete study of $ArSO_3$ established a symmetric top structure. There is little reason to expect a profound structural difference in $KrSO_3$.

It is of interest to compare the Ar and Kr complexes of SO_3 with those of ClF. Table II lists the induced dipole moment for these four systems. For both SO_3 and ClF, the induced moment is greater for the Kr complex than for the Ar complex. For both Ar and Kr, the induced moment is greater for the SO_3 complex than for the corresponding ClF complex. The ratio of polarizabilities of Kr and Ar is 1.51. Novick *et al.*[4] have pointed out that this is close to the ratio of induced electric dipole moments of KrClF and ArClF, namely,

TABLE I. Observed radio frequency transitions in $KrSO_3$.

Frequency (MHz)	E (V/cm)	J	K
1.33(3)	100.73	6	±3
1.89(3)	100.73	5	±3
2.82(3)	100.73	4	±3
4.66(3)	100.61	3	±3

 0021-9606/81/074211-02$01.00